Max Planck-Institut
für Quantenoptik
BIBLIOTHEK
D-8046 Garching

Handbibliothek
MPQ

Space charge effects on ion pinhole images of laser-produced plasmas

Yasukazu Izawa*

MPQ 53 October 1981

MPQ-Report
53

MPQ

MAX-PLANCK-INSTITUT FÜR QUANTENOPTIK
8046 GARCHING BEI MÜNCHEN

MAX-PLANCK-INSTITUT FÜR QUANTENOPTIK

Space charge effects on ion pinhole images of laser-produced plasmas

Yasukazu Izawa*

MPQ 53 October 1981

Max-Planck-Institut
für Quantenoptik
BIBLIOTHEK
D-8046 Garching

* On leave from Institute of Laser Engineering,
Osaka University, Japan

D-8046 Garching bei München

Abstract:

Fast ion pinhole pictures of laser-produced plasmas were obtained on C-N film with a resolution close to the theoretical limit set by the camera geometry and pinhole diameter. This result was obtained in cases where the pinhole was at a sufficiently large distance from the laser-produced plasma ion source and the ion distribution was filtered by thin Al filters. When these precautions were not met the camera resolution was found to be degraded, possibly by space charge effects arising in the pinhole.

I. Introduction

Ion pinhole imaging is a diagnostic technique of interest for the study of laser-produced plasmas /1,2/. However, as pointed out by Gitomer and Brysk /3/, the resolution of this technique may be limited by space charge effects. These space charge effects arise on passage of the expanding plasma through the pinhole, where part of the plasma electrons are lost to the wall. The plasma leaves the pinhole with a net charge and the ion trajectories deviate from straight lines under the influence of the electric field produced by this charge. This results in a reduction of resolution which becomes more severe with increasing plasma density in the pinhole plane.

In this report we describe test results obtained with a pinhole camera used for ion imaging of a laser-produced plasma. We analyze the results in terms of space charge effects following the analysis of Gitomer and Brysk /3/.

II. Experimental set-up

The experimental arrangement is shown in Fig. 1. A laser beam with an energy of 100 J in 300 ps (FWHM) from the Asterix III iodine laser was focussed on a plastic foil target with a thickness of 2 µm. The focal spot diameter was 60 µm, corresponding to an intensity on target of 6×10^{15} W/cm^2.

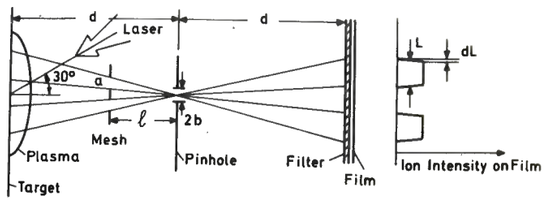

$L = \frac{d}{\ell} a$

$dL = \frac{d+\ell}{\ell} b$

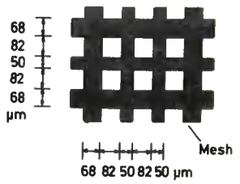

Fig. 1 Experimental arrangement

We used two ion pinhole cameras with different plasma-to-pinhole distances (5 cm and 15 cm), but the same magnification (x 1). A copper mesh, with a mesh size of 82 x 82 µm (open area), was introduced between the target and the pinhole. An image of the mesh backlighted by fast ions from the target was recorded on Kodak LR - 115 type I cellulose nitrate (C-N) film. Pinholes with diameters of 12.5 µm and 25 µm in 20 µm thick nickel foils were used.

The ideal ion intensity distribution (i.e. without space-charge broadening) is also sketched in Fig. 1. Without space-charge broadening the mesh should be imaged with a resolution dL determined by the camera geometry and the pinhole diameter.

As we were interested in pictures produced by the fast ions emitted by the target we used a filter in front of the C-N film. The filter consisted of either a 1 µm or a 2 µm thick aluminium film coated directly onto the film. It absorbs fast ions (protons) with energies of less than 110 and 220 keV, respectively.

It is important to have the filter directly in front of the film because otherwise the resolution will be degraded owing to scattering of the ions in the filter. In Al the mean square angular scattering is 195 deg^2/µm (see /4/).

III. Results

Typical images are shown in Fig. 2 (a-c). Figure 2 (a) is an ion image obtained with uncoated C-N film; (b) and (c) were obtained with 1 and 2 µm Al filters coated onto the film. The ion intensity distributions along the solid line in the photographs are also shown. In Fig. 2(d) and (e), the solid and the dotted line indicate the ideal and the measured distributions, respectively. Both cases show a considerable loss of resolution compared with the calculated distribution.

We analyze the results following Gitomer and Brysk /3/. In the limit of weak ion deflection by the space charge field, the beam radius r at the film is related to the pinhole radius b by the following equation:

$$\ln(r/b) = \frac{e^2}{4}\left(\frac{Z N_2}{m_i \varepsilon_0}\right) T^2 \qquad (1 \leq r/b \leq 1.37) \qquad (1)$$

Here $e, \varepsilon_0, m_i, Z, N_2$ and T are the electron charge, free space permittivity ion mass, ion charge number, space charge number density and transit time from the pinhole to the film.

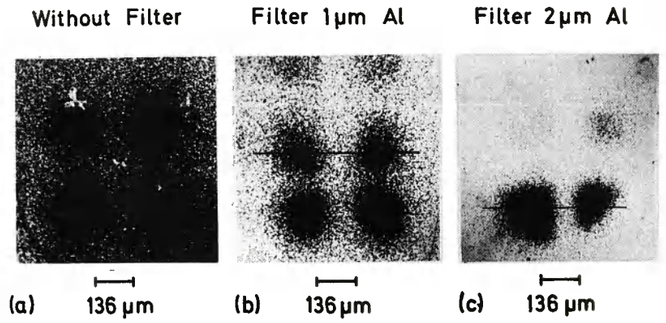

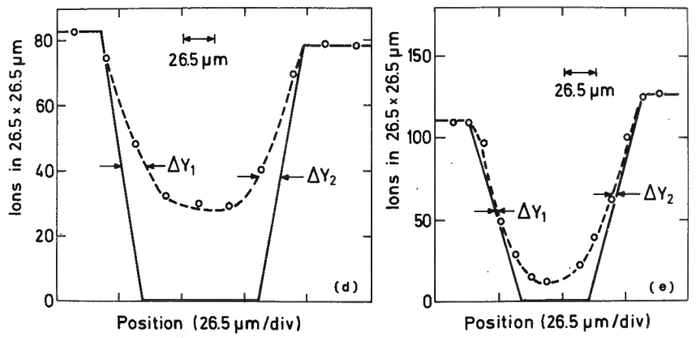

Fig. 2 Fast ion images of the mesh (a, b, c) and ion intensity distributions along the solid line (d, e).
(a) : d = 15 cm, l = 7.5 cm, b = 6.25 μm, no ion filter.
(b) and (d): d = 15 cm, l = 7.5 cm, b = 6.25 μm,
1 μm Al ion filter
(c) and (e): d = 5 cm, l = 2 cm, b = 6.25, 2μm Al
ion filter.

The space charge number density is expressed as follows:

$$N_2 = N_1 (1 - r_c^2/b^2) \qquad (2)$$

$$b - r_c = \left(\frac{A e^2}{2\pi \varepsilon_0 m_e}\right)^{1/2} \frac{L}{v} N_1^{1/2} \qquad (3)$$

where L, v and N_1 are the length of the pinhole, ion velocity and number density of charged particles in the pinhole, and r_c is the critical radius at which an electron injected into the pinhole just strikes the far end of the pinhole side wall.

From these equations, the fractional expansion scales as

$$\ln \delta \propto N_1^{3/2} v^{-3} d^2 b^{-1} \qquad (4)$$

where δ = r/b; d = v/T is the distance from the pinhole to the film.

The measured spread $\delta = 1 + (\Delta r_1 + \Delta r_2)/L$ (see Figs. 1 and 2 for definition of L, Δr_1 and Δr_2) is compared with the above scaling as shown in Fig. 3.

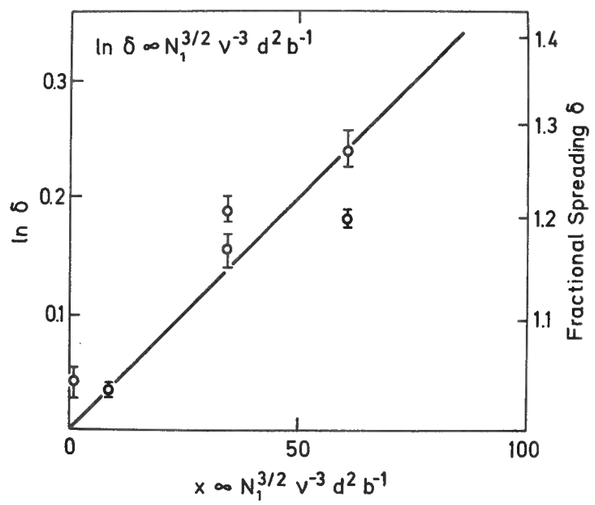

Fig. 3 Scaling of the measured fractional broadening in the ion images

The horizontal scale is proportional to $N_1^{3/2} v^{-3} d^2 b^{-1}$ and is normalized to 1 for the case of d = 15 cm, b = 12.5 μm, $N_1 = 5.6 \times 10^{15}$ m^{-3}, v=6.3 x 10^6m/s (2 μm Al coated CN film). In these calculation we used the data on the energy and angular distributions of the fast ions from plastic foil targets measured in this facility /5/. As is seen in Fig. 3, the scaling of eq.(4) is fairly good.

Two data points at the bottom left of the figure were obtained by using 2 μm Al-coated C-N film. In these cases, the fractional spreading in the ion image is less than 1.05 and is practically negligible for our experimental conditions.

To summarize, we have demonstrated that fast ion pinhole pictures from laser-produced plasmas can be obtained on C-N film with a resolution close to the theoretical limit set by the camera geometry and pinhole diameter. This result was obtained in cases where the pinhole was at a sufficiently large distance from the laser-produced plasma ion source and the ion distribution was filtered by thin Al filters. When these precautions were not met the camera resolution was found to be degraded, possibly by space charge effects arising in the pinhole

Appendix: Fast ion image of a laser-irradiated plastic foil target.

Examples of fast ion images are shown in Fig. A1. These three images were obained in one shot.

Experimental conditions are as follows:

Laser: 89 J in 300 ps

Target: 2 μm plastic foil, 30^o oblique incidence

Camera: d = 15 cm, ion filter: 2 μm Al

a) b = 12.5 μm, direction: target normal

b) b = 6.25 μm, direction: 3^o to target normal

c) b = 6.25 μm, direction: 6^o to target normal

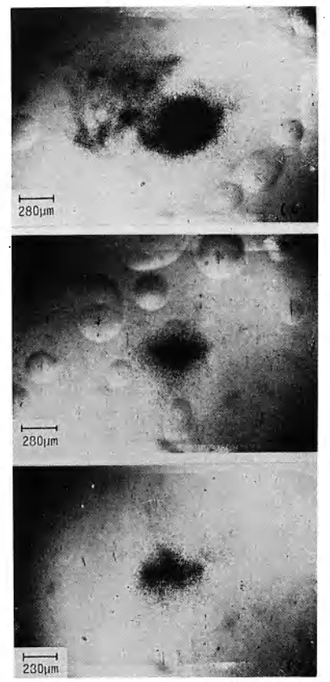

Fig. A.1 Fast ion images ($E_p \geq 210$ keV) of a laser-irradiated plastic foil target.

The following observations may be made on the images:

1) The central part in (a) is overexposed, hence the structure is not clear.

2) Two groups of sources are seen, one in the central part and the other in the surroundings.

3) The image of the central part is asymmetric. The width is $\sim$140 µm horizontally and $\sim$ 110 µm vertically (b). These dimensions are larger than the laser focal spot.

4) Several sources are also observed in the central part (c). This may be caused by filaments in the plasma.

5) Ion emission from the surroundings is not symmetric. This is seen most clearly in (a). The maximum distance from the centre is 900 µm.

6) Crater diameters in the surroundings are different from that in the central part. In the central part the diameter of the craters is $\sim$ 2 µm , in the surroundings less than 1 µm . This may be due to a difference in ion energy or species between the two sources.

7) Defects 200 - 300 µm in diameter as seen in Fig. A.1a) and b) are due to a separation of the C-N layer from the base of the film.

This type of defect is only observed after etching of a 2 µm Al coated film. It is not clear whether it comes from the coating or etching process. After exposure, the C-N film is etched in 2.5 N sodium hydroxide for 25 min at 60° C. In the etching solution, metallic Al reacts violently to form Al $(OH)_3$. But even before the reaction terminates, the Al layer peels off from the C-N film. In order to avoid these defects, it is suggested that the Al filter be removed in a cold etching solution, in which the reaction rate is lower.

References

/1/ V.W. Slivinsky, K.M. Brooks, H.G. Ahlstrom, E.K. Storm, H.N. Kornblum, and G.R. Leipelt, Appl. Phys. Lett. 30, 555 (1977)

/2/ D.C. Slater, Appl. Phys. Lett. 31, 196 (1977)

/3/ S.J. Gitomer and H. Brysk, Appl. Phys. Lett. 32, 616 (1978)

/4/ J.P. Biersack et al., Tables of Electronic and Nuclear Stopping Powers and Energy Straggling for Low Energy Ions, Hahn-Meitner-Institut für Kernforschung, Berlin, June 1975.

/5/ G.D. Tsakiris, K. Eidmann, R. Petsch, and R. Sigel, Phys. Rev. Lett. 46, 1202 (1981)